

Ultrafast Excited State Dynamics of Pt(II) Chromophores Bearing Multiple Infrared Absorbers

Elena A. Glik,[†] Solen Kinayyigit,[†] Kate L. Ronayne,[‡] Michael Towrie,[‡] Igor V. Sazanovich,[§] Julia A. Weinstein,^{*,§} and Felix N. Castellano^{*,†}

Department of Chemistry and Center for Photochemical Sciences, Bowling Green State University, Bowling Green, Ohio, 43403, Laser for Science Facility, Photon Science Department, Rutherford Appleton Laboratory, Science and Technology Facilities Council, Chilton, OX11 0QX, U.K., and Department of Chemistry, University of Sheffield, Sheffield S3 7HF, U.K.

Received April 1, 2008

The paper reports the synthesis, structural characterization, electrochemistry, ultrafast time-resolved infrared (TRIR) and transient absorption (TA) spectroscopy associated with two independent d⁸ square planar Pt(II) diimine chromophores, Pt(dnpeppy)Cl₂ (**1**) and Pt(dnpeppy)(C≡Cnaph)₂ (**2**), where dnpeppy = 4,4'-(CO₂CH₂-^tBu)₂-2,2'-bipyridine and C≡Cnaph = naphthylacetylide. The neopentyl ester substitutions provided markedly improved complex solubility relative to the corresponding ethyl ester which facilitates synthetic elaboration as well as spectroscopic investigations. Following 400 nm pulsed laser excitation in CH₂Cl₂, the 23 cm⁻¹ red shift in the ν_{C=O} vibrations in **1** are representative of a complex displaying a lowest charge-transfer-to-diimine (CT) excited state. The decay kinetics in **1** are composed of two time constants assigned to vibrational cooling of the ³CT excited-state concomitant with its decay to the ground state (τ = 2.2 ± 0.4 ps), and to cooling of the formed vibrationally hot ground electronic state (τ = 15.5 ± 4.0 ps); we note that an assignment of the latter to a ligand field state cannot be excluded. Ultrafast TA data quantitatively support these assignments yielding an excited-state lifetime of 2.7 ± 0.4 ps for the ³CT excited-state of **1** and could not detect any longer-lived species. The primary intention of this study was to develop a Pt^{II} complex (**2**) bearing dual infrared spectroscopic tags (C≡C attached to the metal and C=O (ester) attached to the diimine ligand) to independently track the movement of charge density in different segments of the molecule following pulsed light excitation. Femtosecond laser excitation of **2** in CH₂Cl₂ at 400 nm simultaneously induces a red-shift in both the ν_{C=O} (-30 cm⁻¹) and the ν_{C≡C} (-61 cm⁻¹) vibrations. The TRIR data in **2** are consistent with a charge transfer assignment, and the significant decrease of the energy of the ν_{C≡C} vibration suggests a considerable contribution from the acetylide ligands in the highest occupied molecular orbital. Therefore, we assign the lowest energy optical transitions in **2** as a combination of metal-to-ligand and ligand-to-ligand charge transfers. The excited-state of **2** is emissive at RT, with an emission maximum at 715 nm, quantum yield of 0.0012, and lifetime of 23 ns.

Introduction

A combination of transition metal complexes with selected organic chromophores has generated new molecules and materials that exhibit a wide range of fundamentally interesting and potentially useful excited-state properties.^{1,2} Since their original description in 1994,³ square planar platinum(II)

complexes and materials bearing arylacetylide units have demonstrated promise in a wide range of applications including nonlinear transmission,^{4,5} electroluminescence,⁶ gaseous (vapo)chromic and solution-based chemical sens-

* To whom correspondence should be addressed. E-mail: castell@bgsu.edu (F.N.C.), julia.weinstein@sheffield.ac.uk (J.A.W.)

[†] Bowling Green State University.

[‡] Science and Technology Facilities Council.

[§] University of Sheffield.

(1) Castellano, F. N.; Pomestchenko, I. E.; Shikhova, E.; Hua, F.; Muro, M. L.; Rajapakse, N. *Coord. Chem. Rev.* **2006**, *250*, 1819–1828.

(2) Yam, V. W.-W. *Acc. Chem. Res.* **2002**, *35*, 555–563.

(3) Chan, C.-W.; Cheng, L.-K.; Che, C.-M. *Coord. Chem. Rev.* **1994**, *132*, 87–97.

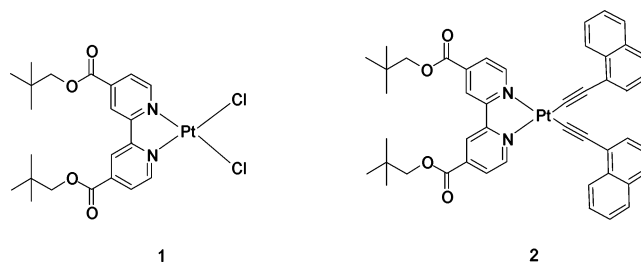
(4) Sun, W.; Wu, Z.-X.; Yang, Q.-Z.; Wu, L.-Z.; Tung, C.-H. *Appl. Phys. Lett.* **2003**, *82*, 850–852.

(5) Guo, F.; Sun, W.; Liu, Y.; Schanze, K. *Inorg. Chem.* **2005**, *44*, 4055–4065.

ing,^{7–11} singlet oxygen photosensitizing,^{12,13} and photocatalysis.^{14–17} Chromophores based on Pt(LL)(C≡CR)₂ and Pt(LLL)(C≡CR), where LL and LLL are substituted diimine or triimine ligands like 2,2'-bipyridine or 2,2',2''-terpyridine and R is typically a substituted alkyl or aryl species, are currently being developed by our groups as well as others.^{1–23} The lowest energy absorption bands in these complexes are generally attributed to Pt→LL or Pt→LLL charge transfer (CT) transitions, with sizable π -contributions from the acetylide ligand(s).^{1,18,19,23} In most instances, the ${}^3\pi\text{-}\pi^*$ states associated with the acetylide and/or LL/LLL substituents are so high in energy that the excited-state behavior is completely dictated by decay of the ${}^3\text{CT}$ level, yielding charge transfer based emission. Through judicious selection of acetylide subunit, acetylide ligand-localized ${}^3\pi\text{-}\pi^*$ excited states with their own distinct spectroscopic properties can be sensitized

in these structures.^{1,18} It has also been shown that the nature of the diimine or triimine ligand and the σ -donating ability of the acetylide moieties can be used to significantly modify the optical and electrochemical properties of the charge transfer state.^{1–23}

While time-resolved emission and absorption have been extensively utilized to elucidate excited-state dynamics in Pt(II) polyimine acetylide structures, time-resolved infrared (TRIR) spectroscopy has only been applied to Pt^{II} diimine bis(acetylide) complexes in one study to date.²⁰ The previous step-scan FTIR investigation revealed that in Pt^{II} complexes with a lowest energy ${}^3\text{CT}$ excited state, namely, Pt(4,4',5,5'-tetra-methyl-2,2'-bpy)(-C≡C-C₆H₄-CH₃)₂ and Pt(dbbpy)(-C≡C-C₆H₄-CH₃)₂, a shift in the $\nu_{\text{C}\equiv\text{C}}$ band to higher frequency (+30–35 cm⁻¹) relative to the ground-state was observed. This was interpreted as being consistent with the metal-to-ligand charge transfer (MLCT) character of the excited state, that is, a decrease in electron density around the metal center as a result of charge transfer diminishes the extent of Pt-C≡C π -backbonding which increases the bond order of the -C≡C- bonds. In contrast, when the lowest energy excited-state in a related Pt^{II} complex Pt(dbbpy)(-C≡C-C₆H₄-NO₂)₂ was believed to be of ${}^3\pi\text{-}\pi^*$ nature, the observed IR frequency shift was extremely small, consistent with little or no charge transfer influence on the C≡C bonds in the excited state. This study exploited the use of a single IR spectroscopic tag (the C≡C bonds) to reveal the nature of the excited state, reminiscent of analogous studies where C=O vibrations are used to probe the nature of Re(I) excited states.^{24,25} It has also been shown that diimine ligands containing either one or two ester units are effective IR spectroscopic tags for charge transfer excited-state characterization.^{26–28} In these instances, the ester C=O stretching frequency (~1730 cm⁻¹) shifts to lower energy in the MLCT excited state, resulting from a decrease in the C=O bond order as a result of populating the antibonding π^* orbital on the ester-containing ligand.



- (6) Chan, S.-C.; Chan, M. C. W.; Wang, Y.; Che, C.-M.; Cheung, K.-K.; Zhu, N. *Chem.—Eur. J.* **2001**, *7*, 4180–4190.
- (7) Lu, W.; Chan, M. C. W.; Zhu, N.; Che, C.-M.; He, Z.; Wong, K.-Y. *Chem.—Eur. J.* **2003**, *9*, 6155–6166.
- (8) (a) Yam, V. W.-W.; Tang, R. P.-L.; Wong, K. M.-C.; Cheung, K.-K. *Organometallics* **2001**, *20*, 4476–4482. (b) Lo, H.-S.; Yip, S.-K.; Wong, K. M.-C.; Zhu, N.; Yam, V. W.-W. *Organometallics* **2006**, *25*, 3537–3540.
- (9) Yang, Q.-Z.; Wu, L.-Z.; Zhang, H.; Chen, B.; Wu, Z.-X.; Zhang, L.-P.; Tung, C.-H. *Inorg. Chem.* **2004**, *43*, 5195–5197.
- (10) Wong, K. M.-C.; Tang, W.-S.; Lu, X.-X.; Zhu, N.; Yam, V. W.-W. *Inorg. Chem.* **2005**, *44*, 1492–1498.
- (11) Wong, K. M.-C.; Yam, V. W.-W. *Coord. Chem. Rev.* **2007**, *251*, 2477–2488.
- (12) Zhang, D.; Wu, L.-Z.; Yang, Q.-Z.; Li, X.-H.; Zhang, L.-P.; Tung, C.-H. *Org. Lett.* **2003**, *5*, 3221–3224.
- (13) Yang, Y.; Zhang, D.; Wu, L.-Z.; Chen, B.; Zhang, L.-P.; Tung, C.-H. *J. Org. Chem.* **2004**, *69*, 4788–4791.
- (14) Zhang, D.; Wu, L.-Z.; Zhou, L.; Han, X.; Yang, Q.-Z.; Zhang, L.-P.; Tung, C.-H. *J. Am. Chem. Soc.* **2004**, *126*, 3440–3441.
- (15) Du, P.; Schneider, J.; Jarosz, P.; Eisenberg, R. *J. Am. Chem. Soc.* **2006**, *128*, 7726–7727.
- (16) Du, P.; Schneider, J.; Jarosz, P.; Zhang, J.; Brennessel, W. W.; Eisenberg, R. *J. Phys. Chem. B* **2007**, *111*, 6887–6894.
- (17) (a) James, S. L.; Younus, M.; Raithby, P. R.; Lewis, J. J. *Organomet. Chem.* **1997**, *543*, 233–235. (b) Adams, C. J.; James, S. L.; Liu, X.; Raithby, P. R.; Yellowless, L. J. *J. Chem. Soc., Dalton Trans.* **2000**, 63–67.
- (18) (a) Pomestchenko, I. E.; Luman, C. R.; Hissler, M.; Ziessel, R.; Castellano, F. N. *Inorg. Chem.* **2003**, *42*, 1394–1396. (b) Pomestchenko, I. E.; Castellano, F. N. *J. Phys. Chem. A* **2004**, *108*, 3485–3492. (c) Danilov, E. O.; Pomestchenko, I. E.; Kinayyigit, S.; Gentili, P. L.; Hissler, M.; Ziessel, R.; Castellano, F. N. *J. Phys. Chem. A* **2005**, *109*, 2465–2471. (d) Hua, F.; Kinayyigit, S.; Cable, J. R.; Castellano, F. N. *Inorg. Chem.* **2005**, *44*, 471–473. (e) Hua, F.; Kinayyigit, S.; Cable, J. R.; Castellano, F. N. *Inorg. Chem.* **2006**, *45*, 4304–4306. (f) Hua, F.; Kinayyigit, S.; Rachford, A. A.; Shikhova, E. A.; Goeb, S.; Cable, J. R.; Adams, C. J.; Kirschbaum, K.; Pinkerton, A. A.; Castellano, F. N. *Inorg. Chem.* **2007**, *46*, 8771–8783. (g) Goeb, S.; Rachford, A. A.; Castellano, F. N. *Chem. Commun.* **2008**, 814–816. (h) Rachford, A. A.; Goeb, S.; Castellano, F. N. *J. Am. Chem. Soc.* **2008**, *130*, 2766–2767.
- (19) Adams, C. J.; Fey, N.; Weinstein, J. A. *Inorg. Chem.* **2006**, *45*, 6105–6107.
- (20) Whittle, C. E.; Weinstein, J. A.; George, M. W.; Schanze, K. S. *Inorg. Chem.* **2001**, *40*, 4053–4062.
- (21) (a) Hissler, M.; Connick, W. B.; Geiger, D. K.; McGarrah, J. E.; Lipa, D.; Lachicotte, R. J.; Eisenberg, R. *Inorg. Chem.* **2000**, *39*, 447–457. (b) McGarrah, J. E.; Kim, Y.-J.; Hissler, M.; Eisenberg, R. *Inorg. Chem.* **2001**, *40*, 4510–4511. (c) Wadas, T. J.; Lachicotte, R. J.; Eisenberg, R. *Inorg. Chem.* **2003**, *42*, 3772–3778. (d) Chakraborty, S.; Wadas, T. J.; Hester, H.; Schmehl, R.; Eisenberg, R. *Inorg. Chem.* **2005**, *44*, 6865–6878.
- (22) Yang, Q.-Z.; Wu, L.-Z.; Wu, Z.-X.; Zhang, L.-P.; Tung, C.-H. *Inorg. Chem.* **2002**, *41*, 5653–5655.
- (23) (a) Yam, V. W.-W.; Wong, K. M.-C.; Zhu, N. *J. Am. Chem. Soc.* **2002**, *124*, 6506–6507. (b) Yam, V. W.-W.; Wong, K. M.-C.; Zhu, N. *Angew. Chem., Int. Ed.* **2003**, *42*, 1400–1403.

The present study combines the two approaches from above where the newly synthesized **2**, Pt(dnpebpy)(C≡Cnap)₂, contains both C≡C and C=O spectroscopic tags positioned on opposite ends of the molecule to independently

- (24) George, M. W.; Turner, J. J. *Coord. Chem. Rev.* **1998**, *177*, 201–217.
- (25) Schoonover, J. R.; Strouse, G. F. *Chem. Rev.* **1998**, *98*, 1335–1355.
- (26) Chen, P.; Omberg, K. M.; Kavaliunas, D. A.; Treadway, J. A.; Palmer, R. A.; Meyer, T. J. *Inorg. Chem.* **1997**, *36*, 954–955.
- (27) Omberg, K. M.; Smith, G. D.; Kavaliunas, D. A.; Chen, P.; Treadway, J. A.; Schoonover, J. R.; Palmer, R. A.; Meyer, T. J. *Inorg. Chem.* **1999**, *38*, 951–956.
- (28) Weinstein, J. A.; Grills, D. C.; Towrie, M.; Matousek, P.; Parker, A. W.; George, M. W. *Chem. Commun.* **2002**, 382–383.

track the redistribution of charge density following photo-excitation. Importantly, these IR frequencies are in regions of the spectrum that are essentially free from other functional group vibrations. Compound **1**, Pt(dnpeppy)Cl₂, models changes in $\nu_{C=O}$ resulting from the formation of the charge-transfer-to-diimine excited-state of prevalently MLCT character, which spectroscopic response can be readily compared to the analogous Pt(II),²⁸ Ru(II),^{26,27} and Re(I)²⁹ complexes already presented in the literature. The combined picosecond TRIR difference spectra from **1** and **2** revealed red shifts in $\nu_{C=O}$ (compounds **1** and **2**) and $\nu_{C\equiv C}$ (compound **2**), consistent with charge transfer assignments in both complexes. The negative shift of $\nu_{C\equiv C}$ in **2** results from significant acetylide ligand character in the highest occupied molecular orbital (HOMO) which leads to a lowering of C≡C bond order upon charge transfer to the dnpeppy ligand, an assignment readily confirmed by the concomitant red shift observed in the C=O bonds in the excited-state of both molecules. The combined TA and TRIR study allowed us to assign the nature of the lowest excited-state in **1** and **2**, and to follow the dynamics of their charge transfer excited states.

Experimental Section

General Information. All reactions were carried out under an inert dry argon atmosphere using standard techniques. Triethylamine (Aldrich Chemical Co.) and diisopropylamine (Aldrich Chemical Co.) were freshly distilled over CaH₂. CH₂Cl₂ (EMD Chemicals) 1-ethynyl-naphthalene ($\nu_{C\equiv C} = 2100\text{ cm}^{-1}$, neat) was distilled under reduced pressure immediately prior to the reaction. All other reagents from commercial sources were used as received. 4,4'-Dimethyl-2,2'-bipyridine, neopentyl alcohol, and copper(I) iodide were commercially available from Aldrich Chemical Co. K₂PtCl₄ and anhydrous benzene were obtained from Alfa Aesar. Chromatographic purification was performed using Silica Gel 60 or aluminum oxide standardized and deactivated with 6% H₂O by weight and a mixture of CH₂Cl₂/CH₃OH (100:1), increasing gradually the polarity of the eluent. All solvent mixtures were given in a v/v ratio. The 300 MHz ¹H NMR spectra were recorded on Bruker Advance Spectrometer at room temperature with perdeuterated chloroform with 0.05% TMS as an internal reference. All splitting patterns were assigned as s (singlet), d (doublet), dd (doublet of doublets), t (triplet), and m (multiplet). MALDI-TOF mass spectra were measured by a Bruker-Daltonics Omnistar Spectrometer; the MALDI matrices were 1,8,9-trihydroxyanthracene for **1** and α -cyano-4-hydroxycinnamic acid for **2**. GC-MS were obtained on a Shimadzu QP5050A spectrometer. FT-IR spectra were taken with a Thermo Nicolet IR-200 Spectrometer equipped with an ATR crystal (BGSU), and with a Perkin-Elmer SpectrumOne FTIR spectrometer (Sheffield).

Preparations. Pt(DMSO)₂Cl₂,³⁰ Pt(dnpeppy)Cl₂,³¹ and Pt(dnpeppy)(CCnaph)₂^{17,18b} were prepared using modified procedures previously described, yielding satisfactory mass and ¹H NMR data. 4,4'-Dicarboxy-2,2'-bipyridine (dcb) was prepared according to the literature procedure.³²

4,4'-Dineopentylester-2,2'-bipyridine (dnpeppy). 4,4'-Dicarboxy-2,2'-bipyridine (2.1 g, 8.6 mmol) was suspended in SOCl₂ (32 mL, 172 mmol) and was refluxed under argon until complete solubilization occurred (~20 h).³³ The excess SOCl₂ was removed by argon purging and the remaining residue was dried under vacuum (88% yield). Neopentyl alcohol (0.74 g, 5.2 mmol) was dissolved in anhydrous benzene (20 mL), and triethylamine (5 mL) was added under argon. A 1.0 g quantity of the diacid chloride was dissolved in benzene (30 mL) and then added dropwise into the alcoholic solution under constant stirring in an argon atmosphere. The reaction mixture was then refluxed for 6 h and then stirred at room temperature overnight. CH₂Cl₂ was added, and the organics extracted with a saturated sodium bicarbonate aqueous solution. The combined organic fractions were dried over MgSO₄, filtered, and rotary evaporated to dryness. The solid was purified by flash chromatography over deactivated alumina using 1% CH₃OH in CH₂Cl₂ as eluent. A white crystalline solid was obtained (63% yield). FT-IR (solid, cm⁻¹): 1719 ($\nu_{C=O}$), 1591, 1558, 1457. ¹H NMR (300 MHz, CDCl₃) δ : 8.89 (s, 2H), 8.82 (d, 2H, $J = 4.89$ Hz), 7.84 (dd, 2H, $J = 4.89$ Hz and $J = 1.71$ Hz), 4.15 (s, 4H), 1.00 (s, 18H). EI/MS (70 eV): m/z 384.

Pt(dnpeppy)Cl₂ (1). Pt(DMSO)₂Cl₂ (245.5 mg, 0.58 mmol) and dnpeppy (223 mg, 0.58 mmol) in a 80 mL mixture of CH₃OH and CH₂Cl₂ (3:1) was placed in a pressure vessel and stirred at 40 °C for 4 h. The solvents were removed under vacuum and the solid recrystallized from CH₂Cl₂/ether, 360 mg (95% yield). Calcd for C₂₂H₂₈Cl₂N₂O₄Pt: C, 40.62; H, 4.34; N, 4.31. Found: C, 40.79; H, 4.26; N, 4.29. FT-IR (solid, cm⁻¹): 1721 ($\nu_{C=O}$), 1596, 1561, 1411. ¹H NMR (300 MHz, CDCl₃) δ : 9.99 (d, 2H, $J = 6.03$ Hz), 8.59 (s, 2H), 8.13 (d, 2H, $J = 6.03$ Hz), 4.18 (s, 4H), 1.09 (s, 18H). MALDI-TOF: 615 ([M⁺ - Cl], 48%), 650 ([M⁺], 16%), 804 ([M⁺ - Cl + matrix], 18%), 840 ([M⁺ + matrix], 18%).

Pt(dnpeppy)(C≡Cnaph)₂ (2). 1-Ethynyl-naphthalene (0.4 mL, 2.81 mmol) was transferred into a degassed 40 mL solution of Pt(dnpeppy)Cl₂ (289.2 mg, 0.444 mmol) in CH₂Cl₂/diisopropylamine (3:1) with a syringe. CuI (20 mg) was added into the reaction mixture under an argon blanket, and the flask was sealed. The mixture was stirred at room temperature for 48 h and chilled in the freezer overnight. All volatile components were evaporated, and the residual orange solid was purified by column chromatography (Silica Gel 60, 100:1 CH₂Cl₂/CH₃OH with gradual increase in the polarity) using CH₂Cl₂/hexane. The yield was 81%. Calcd for C₄₆H₄₂N₂O₄Pt·CH₃OH: C, 61.76; H, 5.07; N, 3.07. Found: C, 61.61; H, 4.97; N, 3.18. FT-IR (solid, cm⁻¹): 2104 ($\nu_{C\equiv C}$), 1729 ($\nu_{C=O}$), 1567, 1471, 1391. ¹H NMR (300 MHz, CDCl₃) δ : 9.97 (d, 2H, $J = 6.55$ Hz), 8.54 (d, 2H, $J = 6.55$ Hz), 8.14 (s, 2H), 7.80–7.78 (m, 4H), 7.67–7.60 (m, 4H), 7.48–7.32 (m, 6H), 3.85 (s, 4H), 0.97 (s, 18H). MALDI-TOF: m/z 882 ([M⁺], 85%), 1108 ([M⁺ + matrix], 15%).

General Photophysical and Electrochemical Measurements. Corrected emission spectra were measured using a FluoroMax-4 spectrofluorimeter (HORIBA Jobin Yvon Inc.). Emission quantum yields were determined relative to [Ru(bpy)₃](PF₆)₂ in deaerated acetonitrile (quantum yield = 0.062³⁴). Emission lifetimes were measured using a nitrogen-pumped broadband dye laser (PTI GL-3300 N₂ laser and PTI GL-301 dye laser) and a Hamamatsu R928 PMT detector wired for fast response, optically coupled to an f/3.4 monochromator.¹⁸ Electrochemical measurements were performed at room temperature in anhydrous CH₂Cl₂ solutions with 0.1 M n-Bu₄NPF₆ (TBAH) as the supporting electrolyte. A platinum

(29) Dattelbaum, D. M.; Omberg, K. M.; Schoonover, J. R.; Martin, R. L.; Meyer, T. J. *Inorg. Chem.* **2002**, *41*, 6071–6079.

(30) Kukushkin, V. Y.; Pombeiro, A. J. L.; Ferreria, C. M. P.; Elding, L. I. *Inorg. Synth.* **2002**, *33*, 189–195.

(31) Hodges, K. D.; Rund, J. V. *Inorg. Chem.* **1975**, *14*, 525–528.

(32) Nathalie, G.; Pierre, V. *J. Org. Chem.* **1992**, *57*, 3046–3051.

(33) Sprintschnik, G.; Sprintschnik, H. W.; Kirsch, P. P.; Whitten, D. G. *J. Am. Chem. Soc.* **1977**, *99*, 4947–4956.

(34) Caspar, J. V.; Meyer, T. J. *J. Am. Chem. Soc.* **1983**, *105*, 5583–5590.

Table 1. Photophysical and Electrochemical Properties of **1** and **2** Measured in CH₂Cl₂ at Room Temperature

	λ_{abs} , nm (ϵ , dm ³ mol ⁻¹ cm ⁻¹)	λ_{em} , ^a nm	τ_{em} , ^b ns	Φ_{em} ^c	k_r , ^d s ⁻¹	k_{nr} , ^e s ⁻¹	$E_{1/2}$, ^f V
1	300 (34412) 340 (7997) 400 (3912) 424 (5497)		<i>g</i>				-1.23; -1.55
2	245 (54962) 320 (36895) 434 (6135) 495 (5909)	715	23	0.0012	5.2×10^4	4.3×10^7	+0.58 (irr); -1.32; -1.53

^a Measured in argon-saturated CH₂Cl₂ solution at room temperature. ^b Emission intensity decay lifetime, ($\pm 5\%$). ^c Quantum yield of emission measured relative to [Ru(bpy)₃](PF₆)₂ ($\Phi_{\text{em}} = 0.062$) in CH₃CN. ^d $k_r = \Phi_{\text{em}}/\tau_{\text{em}}$. ^e $k_{\text{nr}} = (1 - \Phi_{\text{em}})/\tau_{\text{em}}$. ^f Reduction potentials measured in 0.1 M TBAH/CH₂Cl₂ vs Fc⁺/Fc⁰. ^g $\tau_{\text{TA}} = 2.7$ ps.

disk working electrode, platinum wire auxiliary electrode, and a Ag/AgCl (3 M NaCl) reference electrode were used for all the measurements. The ferrocinium/ferrocene couple (Fc^{+/0}) was used as an internal reference. All cyclic voltammograms were recorded with a Bioanalytical Systems Epsilon controller interfaced with a Pentium PC.

TRIR Measurements. The ps-TRIR experiments were performed on solutions of **1** and **2** in CH₂Cl₂, with concentration of approximately 1 mM. The TRIR experiments were carried out at the Central Laser Facility of the Rutherford Appleton Laboratory, STFC, U.K., which has been described in detail elsewhere.³⁵ Briefly, part of the output from a 1 kHz, 800 nm, 150 fs, 1 mJ Ti:Sapphire oscillator/regenerative amplifier was used to pump a white light continuum seeded BBO OPA. The signal and idler produced by this OPA were difference frequency mixed in a type I AgGaS₂ crystal to generate tuneable mid-infrared pulses (ca. 150 cm⁻¹ fwhm, 0.1 μ J). Second harmonic generation of the residual 800 nm light provided 400 nm pulses, which were used to excite the sample (typical excitation energy 3 μ J, focus 150 μ m²). All measurements were carried out at magic angle polarization. Changes in infrared absorption were recorded by normalizing the outputs from a pair of 64-element HgCdTe linear array detectors on a shot-by-shot basis.

Ultrafast Transient Absorption Spectrometry. Femtosecond time-resolved experiments were performed using the spectrometer available at the Ohio Laboratory for Kinetic Spectrometry at BGSU. A detailed description of the home-built ultrafast VIS setup is available elsewhere.³⁶ Samples were excited at 400 nm (~ 130 fs) and probed with a white light continuum generated from 800 nm light in a sapphire plate or CaF₂ crystal. The pump beam was converted to 400 nm excitation wavelength by coupling it into a second-harmonic generator. The energy of the 400 nm pulses was typically ≤ 3 μ J. The solution (CH₂Cl₂ was used as a solvent in all experiments) was pumped through a 2 mm thick quartz flow cell (Starna Cells) at a rate of 120 mL/min. The absorption of the sample at the excitation wavelength was 0.3–0.8 as measured in the 2 mm cell. UV–vis absorbance spectra were recorded before and after each TA experiment to verify that the samples did not decompose.

Results and Discussion

Syntheses. Given the successful application of TRIR spectroscopy to Pt(CO₂Et₂bpy)Cl₂,²⁸ we initially prepared the 4,4'-diethylester-2,2'-bipyridine version of compound **2**, Pt(CO₂Et₂bpy)(C \equiv Cnap)₂. Unfortunately, this complex was

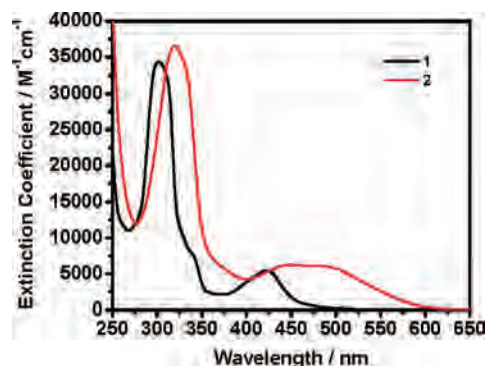


Figure 1. UV–vis absorption spectra of **1** (black line) and **2** (red line) recorded in CH₂Cl₂ at room temperature.

largely insoluble in most organic solvents rendering all TRIR measurements virtually impossible. We circumvented this limitation by preparing a more hydrophobic ester, and the solubility of compound **1** is indeed quite superior to Pt(CO₂Et₂bpy)Cl₂; therefore, we used **1** as a synthon in the preparation of **2**. Esterification of the 4,4'-diacidchloride of 2,2'-bipyridine with neopentyl alcohol in the presence of triethylamine in anhydrous benzene proceeded quite smoothly, yielding the desired ligand which was characterized by ¹H NMR, EI-MS, and FTIR. The highly soluble target complex **1** was synthesized in high yield from Pt(DMSO)₂Cl₂³⁰ and the dnepbpy ligand in CH₂Cl₂ at room temperature. Compound **2** was synthesized using well-established literature methods,^{17,18b} from compound **1** and excess 1-ethynyl-naphthalene in the presence of CuI and diisopropylamine. Both metal complexes were structurally characterized by ¹H NMR, MALDI-TOF MS, elemental analysis, and FTIR.

Photophysical and Electrochemical Properties. Some relevant room-temperature electrochemical and spectroscopic data determined for **1** and **2** are collected in Table 1.

The ground-state absorption spectra of **1** and **2** measured in dichloromethane are displayed in Figure 1. The low-energy absorption band with maximum at 424 nm and extinction coefficient around 5500 M⁻¹ cm⁻¹ in the spectrum of **1** is assigned to charge-transfer-to-diimine transitions of prevalently MLCT character.²⁸ On the basis of the negative solvatochromic behavior observed for **2** (Supporting Information, Figure S1) and previous studies of structurally related Pt^{II} complexes,^{1,18–21} the low-energy bands with maxima near 440 and 495 nm in **2** are assigned to the Pt→diimine CT transitions with significant contributions from the π -orbitals of the acetylide ligands. The high-energy bands centered at 300 nm (in **1**) and 320 nm (in **2**) with extinction coefficients

(35) Towrie, M.; Grills, D. C.; Dyer, J.; Weinstein, J. A.; Matousek, P.; Barton, R.; Bailey, P. D.; Subramaniam, N.; Kwok, W. M.; Ma, C.; Phillips, D.; Parker, A. W.; George, M. W. *Appl. Spectrosc.* **2003**, *57*, 367–380.

(36) Gentili, P. L.; Danilov, E.; Ortica, F.; Rodgers, M. A. J.; Favaro, G. *Photochem. Photobiol. Sci.* **2004**, *3*, 886–891.

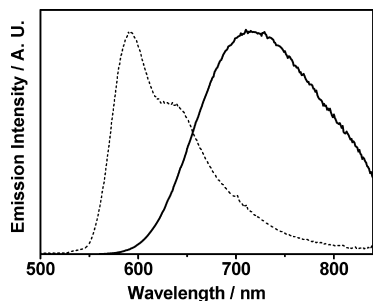


Figure 2. Corrected static emission spectra of **2** measured in degassed CH_2Cl_2 ($\lambda_{\text{ex}} = 470 \text{ nm}$) at room temperature (solid line) and at 77 K in a 2-MeTHF matrix (dashed line).

of $\sim 35000 \text{ M}^{-1} \text{ cm}^{-1}$ correspond to diimine- and acetylide-based intraligand $\pi\text{-}\pi^*$ transitions and do not exhibit any noteworthy charge-transfer character. The latter assignment is consistent with the invariance of the band position to solvent polarity (Supporting Information, Figure S1).

The corrected emission spectrum of **2** in degassed CH_2Cl_2 solution is broad and structureless, with a maximum at 715 nm (Figure 2). The excitation spectrum matches the absorption spectrum (Supporting Information, Figure S1), confirming that emission originates from the parent compound. In an optically dilute (10^{-6} M) degassed solution of **2** in CH_2Cl_2 the photoluminescence quantum yield is 0.0012; the emission decay is monoexponential, with a lifetime of 23 ns (Supporting Information, Figure S2). On the basis of the large Stokes shift, the width of the profile, and the 23 ns lifetime, the emission is assigned as triplet charge transfer in nature. Based upon our previous studies on related diimine and diphosphine Pt(II) naphthylacetylide systems, we conclude that the ligand localized triplet state on the $\text{C}\equiv\text{Cnaph}$ subunit does not participate in the room temperature photophysics in **2** since it lies too high in energy relative to the ^3CT excited state.^{18b} The lack of involvement of the intra-acetylide $^3\pi\pi^*$ excited-state is supported by the emission data measured at 77 K in 2-MeTHF. The emission of **2** at 77 K (Figure 2) is characterized by the spectrum with a maximum at 590 nm with poorly resolved structure, and emission lifetime of about $3.5 \mu\text{s}$. These characteristics resemble those of the ^3CT state in other Pt^{II} diimine *bis*-acetylides,^{1,18,20,21} but contrast to those of the emission from intra- $\text{C}\equiv\text{Cnaph}$ $^3\pi\pi^*$ state, which has a well-resolved vibrational structure with the lowest vibrational band centered at 540 nm and possesses a $470 \mu\text{s}$ lifetime at 77 K.^{18b} The presence of low-lying ^3CT state in **2** is not surprising given the fact that esterification of diimine ligands renders low energy CT states in their corresponding metal complexes.³⁷ Pt(dnpebp) Cl_2 (**1**) is nonluminescent at room temperature which can be rationalized as efficient nonradiative decay of the excited-state via a low-lying metal-centered ligand field state.³⁸

Cyclic voltammograms of **1** and **2** exhibited two reversible reductions in degassed 0.1 M TBAH/ CH_2Cl_2 . Because the reduction potentials for both complexes are comparable

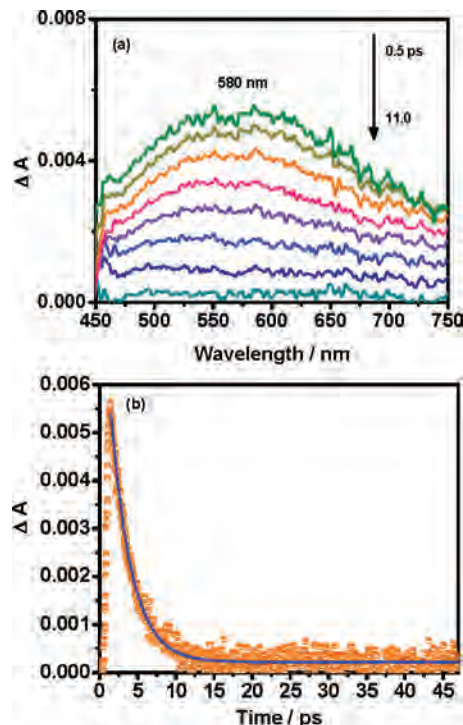


Figure 3. (a) Transient absorption difference spectra of **1** in CH_2Cl_2 , excited at 400 nm ($\sim 130 \text{ fs}$ fwhm), with the delay times specified on the graph. (b) The kinetic trace at 586 nm is displayed along with a superimposed single exponential fit (blue line) with a 2.7 ps lifetime.

(-1.23 ; -1.55 and -1.32 ; -1.53 V , respectively, vs $\text{Fc}^{+/0}$) they must correspond to the sequential addition of electrons to the dnpebp ligand. No oxidation process could be observed for complex **1** because of the limited potential range of the TBAH/ CH_2Cl_2 electrolyte solution. The oxidation wave of **2** is irreversible and assigned to the oxidation of the HOMO which is composed of both Pt and acetylide ligand-based orbitals.^{1,18,21,39,40}

Ultrafast Transient Absorption Spectrometry. Ultrafast time-resolved transient absorption data were collected in an effort to study the excited-state absorption properties of **1** and **2** to facilitate kinetic comparisons with the TRIR data discussed later. In all cases excitation was provided by $\sim 130 \text{ fs}$, 400 nm laser pulses.

Complex 1. Figure 3 presents the TA difference spectra collected at selected delay times following 400 nm excitation ($3 \mu\text{J/pulse}$). The difference spectra are broad, void of strongly absorbing/bleaching features, and extend over the entire visible region ($\lambda_{\text{max}} \approx 580 \text{ nm}$). Kinetic analysis of the ultrafast dynamics at three different wavelengths (481 nm, 538 nm, and 582 nm) yielded monoexponential decays with a lifetime of $2.7 \pm 0.4 \text{ ps}$, assigned to ^3CT excited-state relaxation to the ground state, Figure 3b. It is important to note that when pumping at 340 nm, the dynamics of this decay do not change, yielding an identical time constant of $2.7 \pm 0.2 \text{ ps}$ (Supporting Information, Figure S3b). Because the transient spectrum of **1** is structurally unspecific, a probe

(37) Wacholtz, W. F.; Auerbach, R. A.; Schmehl, R. H. *Inorg. Chem.* **1986**, *25*, 227–234.

(38) McMillin, D. R.; Moore, J. J. *Coord. Chem. Rev.* **2002**, *229*, 113–121.

(39) Zuleta, J. A.; Burberry, M. S.; Eisenberg, R. *Coord. Chem. Rev.* **1990**, *97*, 47–64.

(40) Blanton, C. B.; Murtaza, Z.; Shaver, R. J.; Rillema, D. P. *Inorg. Chem.* **1992**, *31*, 3230–3235.

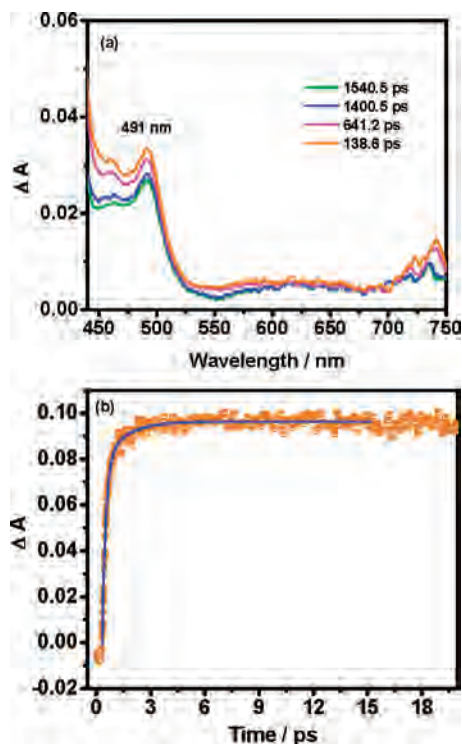


Figure 4. (a) Excited-state absorption difference spectra of **2** in CH_2Cl_2 , excited at 400 nm (~ 130 fs fwhm), with delay times specified on the graph. (b) The kinetic trace at 476 nm. Solid line represent biexponential fit to data.

light continuum generated in a CaF_2 crystal was used to investigate the blue region of the spectrum, see Supporting Information, Figure S3a. As expected for a diimine based CT excited state, a relatively intensive positive transient absorption feature between 350–400 nm and a bleaching signal centered at 424 nm were observed. The positive absorption band below 400 nm is typical for transitions characteristic of one-electron reduced bipyridine.^{18,20,41–43} The negative band observed at 400–445 nm is due to the ground-state bleaching corresponding to the lowest-energy absorption band assigned as the CT-to-diimine transition in Figure 1. This broad transient spectrum decays according to the first order kinetics with the lifetime of 2.7 ps at all examined probe wavelengths (380, 425, and 566 nm); no other longer lived components were detectable. We therefore conclude that the excited-state lifetime of the ^3CT state in **1** is 2.7 ps.

Complex 2. The time-resolved spectral evolution for the naphthylacetylide complex **2** measured after 400 nm excitation ($1 \mu\text{J}/\text{pulse}$) is shown in Figure 4a. The transient is characterized by a relatively intense broadband absorption (440–525 nm) with a maximum at 490 nm and a very weak positive transient stretching across the remainder of the visible region (525–750 nm). These transient features are

largely formed within 200 fs and are believed to be predominately associated with the $^3\text{MLCT}/\text{LLCT}$ (ligand-to-ligand charge transfer) excited state. Further excited-state evolution slightly reduces the transient absorption in the high-energy region of the spectrum; the change in intensity in the red region of the difference spectrum is almost constant with time. The modest signal changes at longer delay times (up to 1.5 ns) are consistent with the 23 ns excited-state lifetime of complex **2** in CH_2Cl_2 , which would be expected to impart measurable decay dynamics on this time scale. The kinetic trace corresponding to the 476 nm probe wavelength is presented in Figure 4b. The data are well modeled to a biexponential function with a sum of two time constants, 200 ± 10 fs and 1.3 ± 0.2 ps. The short time constant resembles that observed previously for the other diimine complexes, for example those of $\text{Re}(\text{I})$ ⁴² and $\text{Ru}(\text{II})$ ⁴³ complexes. The longer time constant is assigned to vibrational relaxation occurring in the triplet excited state, as previously suggested and echoes the interpretations we previously put forth in describing the ultrafast behavior of $\text{Pt}(\text{d}bb\text{py})(\text{C}\equiv\text{CPh})_2$.^{18c} As stated above, there is some additional decay dynamics on longer time scales but instrumental time delay limitations precludes any further kinetic analyses.

Time-Resolved Infrared Spectroscopy. The presence of IR reporters, two ester groups in **1** and **2** and two acetylide groups in **2**, allowed for the application of time-resolved infrared spectroscopy (TRIR) to investigate the nature and dynamics of the excited states in these chromophores. In particular, vectorial charge transfer processes in **2** can be definitively tracked as a result of IR reporters being resident on opposite ends of the molecule. TRIR, a combination of UV pump and fast IR detection, has been broadly used as a powerful probe of the nature of the excited states of coordination compounds,^{24,25,42,44} including several classes of square planar Pt(II) chromophores.^{20,28,45–47}

Complex 1. The ground-state IR spectrum of **1** measured in CH_2Cl_2 at room temperature displays a strong $\nu(\text{CO})$ band at 1733 cm^{-1} (Figure 5b). Upon excitation with a 400 nm, 150 fs laser pulse an instantaneous bleaching of the parent absorption at 1733 cm^{-1} was observed, concomitant with the formation of a new broad $\nu(\text{CO})$ band at about 1710 cm^{-1} as detected at a 1 ps delay time (Figure 5a). Within 100 ps, the bleach and transient features recover back to the baseline. The decrease in the energy of the $\nu(\text{CO})$ vibration observed upon excitation reflects an increase of electronic density on the antibonding $\text{C}=\text{O} \pi^*$ orbital of the ester groups, suggesting that the ester groups of the diimine ligand are coupled with the electronic transition investigated. The shift

(41) (a) Damrauer, N. H.; Cerullo, G.; Yeh, A.; Boussie, T. R.; Shank, C. V.; McCusker, J. K. *Science* **1997**, *275*, 54–57. (b) Yeh, A. T.; Shank, C. V.; McCusker, J. K. *Science* **2000**, *289*, 935–938. (c) McCusker, J. K. *Acc. Chem. Res.* **2003**, *36*, 876–887.
 (42) Liard, D. J.; Busby, M.; Matousek, P.; Towrie, M.; Vlček, A., Jr. *J. Phys. Chem. A* **2004**, *108*, 2363–2369.
 (43) Wallin, S.; Davidsson, J.; Modin, J.; Hammarström, L. *J. Phys. Chem. A* **2005**, *109*, 4697–4704.

(44) (a) Schoonover, J. R.; Bignozzi, C. A.; Meyer, T. J. *Coord. Chem. Rev.* **1997**, *165*, 239–266. (b) Butler, J. M.; George, M. W.; Schoonover, J. R.; Dattelbaum, D. M.; Meyer, T. J. *Coord. Chem. Rev.* **2007**, *251*, 492–514.
 (45) Cooper, T. M.; Blaudeau, J.-P.; Hall, B. C.; Rogers, J. E.; McLean, D. G.; Liu, Y.; Toscano, J. P. *Chem. Phys. Lett.* **2004**, *400*, 239–244.
 (46) Weinstein, J. A.; Blake, A. J.; Davies, E. S.; Davis, A. L.; George, M. W.; Grills, D. C.; Lileev, I. V.; Maksimov, A. M.; Matousek, P.; Mel'nikov, M. Y.; Parker, A. W.; Platonov, V. E.; Towrie, M.; Wilson, C.; Zheligovskaya, N. N. *Inorg. Chem.* **2003**, *42*, 7077–7085.
 (47) Smith, G. D.; Hutson, M. S.; Lu, Y.; Tierney, M. T.; Grinstaff, M. W.; Palmer, R. A. *Appl. Spectrosc.* **2001**, *55*, 637–642.

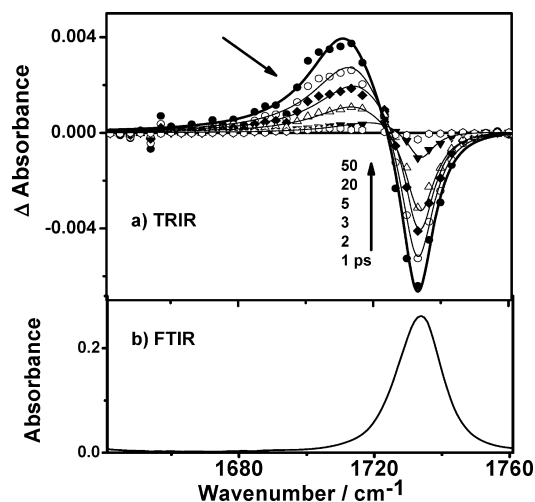


Figure 5. Time-resolved IR spectra of **1** in CH_2Cl_2 at 1, 2, 3, 5, 20, and 50 ps delay after the 400 nm (150 fs, $3 \mu\text{J}$) laser excitation pulse. Solid lines represent 2-band Lorentzian fit of the spectra. The position and fwhm for the parent bleach were fixed according to the FTIR spectrum.

observed in $\nu(\text{CO})$ upon promotion to the excited-state is rather close to that observed previously upon formation of the $^3\text{MLCT}$ state in Ru^{II} and Re^{I} complexes with diimine ligands bearing two ester or two amide groups.^{26,27,48} This observation is consistent with an MLCT assignment of the lowest excited-state in **1**.

The 400 nm excitation corresponds to direct pumping of the ^1CT -to-diimine absorption band of **1**. It has been shown that the intersystem crossing (ISC) process in the $^1\text{MLCT}^*$ state of $[\text{Ru}(\text{bpy})_3]^{2+}$ resulting in the formation of the $^3\text{MLCT}$ state is complete within several tens of femtoseconds.^{41,49} Assuming that the rate of ISC in Pt^{II} complexes would not be considerably slower,^{18c} we assign the TRIR spectrum registered at 1 ps to the ^3CT -to-diimine excited-state in **1**.

It is noteworthy that the decay of the transient band in **1** is accompanied by a shift to higher energies, from 1710 to 1720 cm^{-1} . Such behavior is typical for early relaxation processes associated with the decay of vibrationally “hot” electronic states.⁵⁰ Therefore, the 1710 cm^{-1} vibration detected 1 ps after the excitation pulse likely corresponds to a vibrationally hot CT-to-diimine state of **1**, as was proposed previously for $[\text{Pt}(4,4'-(\text{CO}_2\text{Et})_2-2,2'\text{-bpy})\text{Cl}_2]$.²⁸

The kinetic traces obtained using multi-Lorentzian curve fitting of the spectra at each time delay are shown in Figure 6. The spectral fitting was achieved by fixing the position and FWHM of the ground-state bleach, as determined from the original FTIR spectrum. The transient decay is well modeled by a sum of two single exponential components,

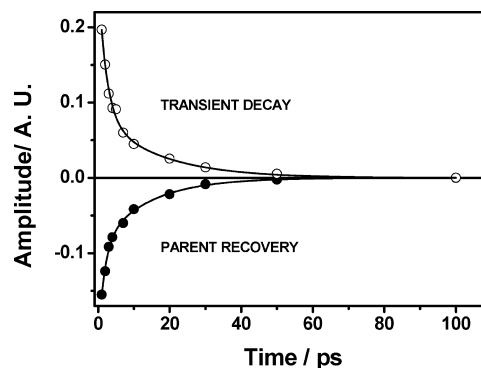


Figure 6. Kinetics of the parent recovery, followed by the 1733 cm^{-1} $\nu(\text{CO})$ in the ground state, and transient decay of **1** in CH_2Cl_2 under 400 nm (150 fs, $3 \mu\text{J}$) laser excitation pulse. Solid lines represent the biexponential fit to the data.

with characteristic lifetimes of $2.2 \pm 0.4 \text{ ps}$ and $15.5 \pm 4.0 \text{ ps}$. These values are very similar to those obtained previously for $\text{Pt}(4,4'-(\text{CO}_2\text{Et})_2-2,2'\text{-bpy})\text{Cl}_2$ from TRIR experiments performed under identical conditions.²⁸ The previously proposed interpretation based solely on TRIR data assigned the $\sim 2 \text{ ps}$ component to the decay of a vibrationally hot MLCT excited state, and the longer component to the decay of the “relaxed” MLCT state to the ground state. This assignment was consistent with the $\sim 2 \text{ ps}$ lifetime of vibrational relaxation which had been reported for the excited state $[\text{Ru}^{\text{III}}(4,4'\text{-diphenyl-2,2'\text{-bpy}^-)_3]^{2+*}$ in CD_3CN ,⁵¹ as well as in $\text{Re}(\text{I})$ complexes.⁵²

In the present work, the TRIR investigation has been complemented by ultrafast transient absorption measurements, Figure 3, which led to an alternative interpretation of the ultrafast dynamics. The 2.2 ps lifetime detected in the TRIR experiments coincides within the experimental error with the value of 2.7 ps obtained in the TA experiments (Figure 3). Intriguingly, the 15.5 ps component in the dynamics of **1** is only observed in the TRIR experiments but not in the transient absorption experiments. Such difference between the TRIR and TA data can be rationalized in terms of the formation of a vibrationally hot ground electronic state which would be silent in transient absorption measurements but would render a signal in the TRIR spectrum. This is not unreasonable considering that the decay of the ^3CT state with a 2 ps lifetime would require a transfer of $25\,000 \text{ cm}^{-1}$ of energy to the vibrational system within a few picoseconds, which is likely to populate a distribution of vibrational levels of the ground electronic state. Thus, the long component (Figure 6) of $15.5 \pm 4.0 \text{ ps}$ in the transient decay and parent recovery registered in the TRIR experiments is attributed to the lifetime of the vibrationally hot ground electronic state, which appears at 1720 cm^{-1} . The formation of vibrationally hot ground states has been documented when the ground-state is populated from an electronic excited state within several picoseconds, consider-

(48) Chen, P. Y.; Palmer, R. A.; Meyer, T. J. *J. Phys. Chem. A* **1998**, *102*, 3042–3047.

(49) (a) Bhasikuttan, A. C.; Suzuki, M.; Nakashima, S.; Okada, T. *J. Am. Chem. Soc.* **2002**, *124*, 8398–8405. (b) Cannizzo, A.; van Mourik, F.; Gawelda, W.; Zgrablic, G.; Bressler, C.; Chergui, M. *Angew. Chem., Int. Ed.* **2006**, *45*, 3174–3176.

(50) (a) Dougherty, T. P.; Heilweil, E. J. *Chem. Phys. Lett.* **1994**, *227*, 19–25. (b) Hamm, P.; Ohline, S. M.; Zinth, W. *J. Chem. Phys.* **1997**, *106*, 519–529. (c) Marks, S.; Cornelius, P. A.; Harris, C. B. *J. Chem. Phys.* **1980**, *73*, 3069–3081. (d) Banno, M.; Iwata, K.; Hamaguchi, H. *J. Chem. Phys.* **2007**, *126*, Article Number 204501. (e) Kondo, M.; Nappa, J.; Ronayne, K. L.; Stelling, A. L.; Tonge, P. J.; Meech, S. R. *J. Phys. Chem. B* **2006**, *110*, 20107–20110.

(51) Damrauer, N. H.; McCusker, J. K. *J. Phys. Chem. A* **1999**, *103*, 8440–8446.

(52) Blanco-Rodríguez, A. M.; Busby, M.; Grădinaru, C.; Crane, B. R.; Di Billo, A. J.; Matousek, P.; Towrie, M.; Leigh, B. S.; Richards, J. H.; Vlček, A., Jr.; Gray, H. B. *J. Am. Chem. Soc.* **2006**, *128*, 4365–4370.

ably faster than intermolecular cooling of either state can occur. The time scale of cooling of vibrationally hot ground states of large molecular systems has been reported to lie in the range from several picoseconds to several tens of picoseconds.⁵³

Overall, a combination of transient absorption and TRIR spectroscopies allowed for the assignment of the 2.2 ps component in the dynamics of **1** to the decay of ³CT that populates a vibrationally hot ground state, in which vibrational cooling with a ~ 15 ps lifetime regenerates the original ground state. These data demonstrate the complementarity of transient electronic and vibrational spectroscopies with respect to information conveyed in relation to the excited-state dynamics. One alternative suggested by a referee is that the 15 ps dynamics relates to a ligand field (LF) excited state. Indeed, it is commonly accepted that the decay of the CT excited-state via a deactivating LF state is responsible for the ultrashort lifetime of the ³CT state in the majority of Pt(diimine)Cl₂ complexes. It is also known that a formation of the LF excited-state is accompanied by a very small change in the IR frequencies.^{44b} It is therefore not unreasonable to suggest that the 15 ps decay time constant associated with $\nu(\text{CO})$ at 1720 cm⁻¹ may relate to the LF state in **1**. Experiments under direct LF-excitation, as well as correlation experiments would be necessary to probe this assignment.

Complex 2. The redistribution of electron density in the excited-state of **2** was monitored using both ester and acetylide IR reporters located on the opposite sides of the molecule. Accordingly, the TRIR experiments were performed in the ranges from 1650 to 1800 cm⁻¹ and from 1950 to 2200 cm⁻¹. The data discussed below were obtained in CH₂Cl₂; virtually identical data were obtained in THF solution, and the corresponding figures are given in the Supporting Information.

Ester region, 1650 to 1800 cm⁻¹. In this region, the ground-state infrared spectrum of **2** in CH₂Cl₂ at room temperature exhibits a $\nu(\text{CO})$ band at 1733 cm⁻¹. There is virtually no difference in the position of $\nu(\text{CO})$ between the Cl complex **1** and the acetylide complex **2**, indicating little influence of the *trans*-disposed ligands on the electron density localized on the ester group in these complexes in their ground electronic state.

Excitation at 400 nm in **2** leads to an instantaneous bleaching of the $\nu(\text{CO})$ parent absorption at 1733 cm⁻¹, concomitantly with the formation of a new band at about 1703 cm⁻¹. Picosecond TRIR spectra recorded at several pump–probe delays between 1 and 2500 ps are shown in Figure 7. The negative shift of the $\nu(\text{CO})$ vibration observed in the TRIR spectra (ca. -30 cm⁻¹) is consistent with an increased electron density on the π^* -orbital of the CO group, as anticipated upon promotion to a charge-transfer-to-diimine excited state. The -30 cm⁻¹ shift observed in $\nu(\text{CO})$ upon excitation of **2** at early time delays is rather close to that reported previously for the ³MLCT state in Ru^{II} or Re^I complexes with symmetric

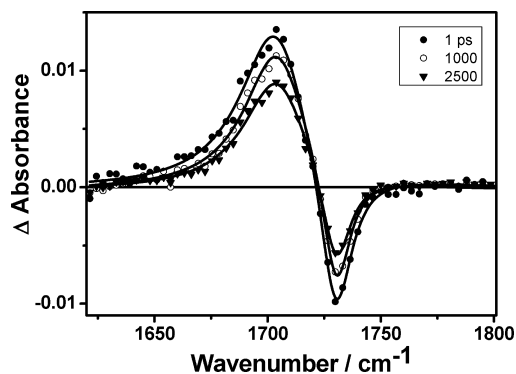


Figure 7. Time-resolved IR spectra of **2** in CH₂Cl₂ at 1, 1000, and 2500 ps delay after the 400 nm laser excitation pulse in the region of the $\nu(\text{CO})$ vibration. Solid lines represent Lorentzian deconvolution of the spectra. For deconvolution, the position and fwhm for the parent bleach were fixed according to the FTIR (± 1 cm⁻¹) at 1733 cm⁻¹. The transient band is at 1703 cm⁻¹.

diimine ligands bearing two ester or two amide groups. This observation suggests that the lowest unoccupied molecular orbital (LUMO) is predominantly localized on the diimine ligand in all cases, with perhaps a small contribution from the metal. This is experimentally consistent with the cyclic voltammetry data discussed earlier (Table 1) where the first two reductions in this complex are indeed diimine ligand based.³⁷

The TRIR spectra were fitted assuming a Lorentzian band shape (solid lines in Figure 7), allowing the determination of the areas of the bleach and transient at each time delay. The position of the transient band remains virtually the same throughout the 1 to 2500 ps time frame investigated. The bandwidth of the transient band has slightly decreased within the first two picoseconds, a phenomenon which we could not follow in detail because of limitations in our instrument time resolution. Consequently, the rate of the vibrational relaxation process was not resolved in this case and no consecutive ultrafast dynamics could be observed. A slightly larger negative shift in $\nu(\text{CO})$ observed in the acetylide complex **2** (-30 cm⁻¹) when compared to its chloro-counterpart **1** (-23 cm⁻¹) implies a somewhat larger increase of electron density on the ester group in the acetylide complex upon promotion to the excited state. Because $\nu(\text{CO})$ is identical for the ground states of **1** and **2**, the difference observed is purely due to delocalization of electron density in the excited state. This could be rationalized in terms of lesser Pt^{II} involvement in the LUMO in the ground-state of **2** and in the singly occupied molecular orbital (SOMO) of **2**⁻.

The -30 cm⁻¹ shift observed in $\nu(\text{CO})$ upon formation of the CT excited-state of **2** is considerably smaller than the -46 cm⁻¹ reported for [Ru(bpy)₂(4-(CO₂Et)-4'-CH₃-2,2'-bpy)]²⁺²⁶ in which the bpy-ligand bears only one ester group. This difference suggests that the electronic density in the CT excited-state of **2** is delocalized over both pyridine rings of the bpy-ester ligand within the first 1 ps after excitation, as has been reported for the Ru^{II}-complex with symmetric ester- and amido-bearing diimine ligands.^{26,27,48} The small decrease in the intensity of the transient signal and parent

(53) Elsaesser, T.; Kaiser, W. *Annu. Rev. Phys. Chem.* **1991**, *42*, 83–107.

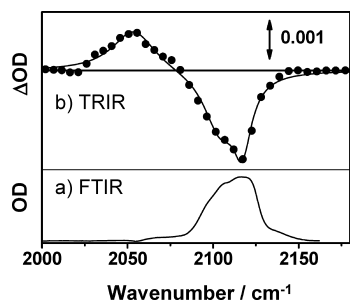


Figure 8. (a) FTIR spectrum of **2** in CH₂Cl₂; (b) Time-resolved IR spectrum of **2** in CH₂Cl₂ at 50 ps delay after the 400 nm laser excitation pulse in the region of $\nu(\text{C}\equiv\text{C})$. Solid line represents Lorentzian fit to the spectra.

bleach by 2500 ps (Figure 3) is consistent with the 23 ns lifetime of **2** determined by transient emission spectroscopy, Table 1 and Supporting Information, Figure S2.

Acetylide region, 1950–2200 cm⁻¹. In this region, the FTIR spectrum of **2** has a $\nu(\text{CC})$ band at 2115 cm⁻¹ (Figure 8a). This feature appears asymmetric because of two unresolved $\nu(\text{CC})$ bands expected from the *bis*-acetylide **2**. The Lorentz fit to the spectrum reveals the presence of two bands, at 2115 and 2102 (sh) cm⁻¹, which appear at somewhat lower energies than those reported previously for Pt(4,4'-X₂-bpy)(CCPh)₂ derivatives (2124 and 2115 cm⁻¹).²⁰

Excitation at 400 nm with a 150 fs laser pulse leads to an instantaneous bleaching of the $\nu(\text{CC})$ parent absorption positioned at 2115 cm⁻¹, concomitantly with the formation of a new broad band at about 2054 cm⁻¹, Figure 8. In principle two bands associated with $\nu(\text{CC})$ are anticipated in the excited-state of **2**. Although those have not been resolved within the resolution of the TRIR apparatus, the presence of two closely spaced vibrations may account for the broadness of the transient IR band observed, Figure 8b; alternatively, one of the bands in the excited-state may lie outside of the range investigated. Similar to the $\nu(\text{CO})$ case, no ultrafast dynamics could be resolved for $\nu(\text{CC})$, because of the low S/N of the data in this region of the spectrum. The difference spectra measured 1 and 2500 ps delays are essentially identical in shape, and the lack of any pronounced decay of the transient band or of the parent bleach recovery is consistent with the 23 ns lifetime of the excited-state in **2**.

The large (-61 cm^{-1}) negative shift in the $\nu(\text{CC})$ reflects a decrease of the electron density on the acetylide ligand and supports the {Pt/acetylide} assignment of the HOMO in **2**. This result is different from that previously observed for closely related Pt(bpy)(CCPh)₂ derivatives,²⁰ in which an *increase* of 30–35 cm⁻¹ in the $\nu(\text{CC})$ upon promotion to the excited-state has been reported, and attributed to the decreased backbonding to the C \equiv C bond from Pt d-orbitals upon formation of an MLCT excited state. Such difference in behavior could be rationalized in terms of the influence of the Naph vs Ph group on the overall delocalization of electron density in the excited state and much larger CC-Naph moiety involvement in the HOMO.^{18b} One may also note that 4,4'-(CO₂-CH₂-*t*Bu)₂-2,2'-bipyridine is more electron accepting than the alkyl-substituted 2,2'-bipyridines used in the previous study. The notion that back-bonding from

the Pt center to the C \equiv C bond is not particularly strong in **2** is evidenced by the fact that the ground-state $\nu(\text{CC})$ is essentially the same for the (diimine)-Pt(CC-Naph)₂ complex and for free naphthylacetylene ($\nu(\text{CC}) = 2100 \text{ cm}^{-1}$). These results show the possibility of fine-tuning of electron density localization in the excited-state by means of variations of the electronic structure of the ground state. An admixture of the IL ³ $\pi\pi^*$ excited-state may in principle also cause a slight downward shift of the $\nu(\text{CC})$ in the excited-state because of the population of the π^* antibonding orbital. However, the emission results discussed above render such contribution unlikely. Incidentally, a negative shift in the $\nu(\text{CC})$ vibration, from 2090 to 2040 cm⁻¹, has been observed upon promotion to the excited-state of related diphosphine Pt^{II} acetylide chromophores⁴⁵ and was interpreted as a reduction of the $-\text{C}\equiv\text{C}-$ bond order in the excited state. Thus, the picosecond TRIR data obtained for **2** support the MLCT/LLCT assignment of its lowest excited state.

Conclusions

The present study investigated the ultrafast excited-state dynamics of two distinct Pt^{II} diimine charge transfer chromophores using complementary TRIR and TA spectroscopic methods. For this purpose, Pt(dnpebpy)Cl₂ (**1**) and Pt(dnpebpy)(CCnaph)₂ (**2**), where dnpebpy = 4,4'-(CO₂CH₂-*t*Bu)₂-2,2'-bipyridine and CCnaph = naphthylacetylide, were prepared and fully characterized. Chromophore **2** possesses ester and acetylide IR reporter groups positioned at the opposite ends of the molecule to allow one to monitor a redistribution of electron density induced by photoexcitation. The lowest excited-state was assigned as MLCT in **1** and as a charge transfer from the HOMO of Pt/acetylide origin to the diimine-based LUMO in **2**. The lifetime of the ³CT state of **1** is extremely short, approximately 2.5 ps. The rapid decay of this ³CT state produces a vibrationally hot ground electronic state, in which vibrational relaxation with a time constant of ~ 15 ps completes the regeneration of the ground state. It shall be noted that an assignment of the ~ 15 ps component to the LF state of **1** cannot be excluded on the basis of the present data. The acetylide chromophore **2** possesses a much longer-lived excited state ($\tau = 23$ ns) in comparison to **1**. Femtosecond laser excitation of **2** in CH₂Cl₂ at 400 nm simultaneously induces a shift to lower energies in both the $\nu_{\text{C}=\text{O}}$ (-30 cm^{-1}) and the $\nu_{\text{C}\equiv\text{C}}$ (-61 cm^{-1}) vibrations. The charge transfer transition from the Pt/acetylide moiety to the diester-substituted bpy ligand in **2** causes a net decrease in the energy of the $\nu(\text{CO})$ of the ester substituents because of a population of π^* -orbital of the C=O groups, and a decrease in energy of the $\nu(\text{CC})$ vibration because of depopulation of the bonding orbitals associated with the C \equiv C bonds. Given that a similar transient red shift (-23 cm^{-1}) is observed for $\nu(\text{CO})$ in the model CT-to-diimine chromophore **1**, the lowest excited-state in **2** can be assigned as MLCT/LLCT in nature.

Acknowledgment. We thank EPSRC, U.K. (GR/T03345 and T03352) for financial support and Rutherford Appleton Laboratory, STFC, U.K. for TRIR beam time. I.V.S. thanks

EU for a Marie Curie Incoming International Fellowship (MIF1-CT-2006-040168). The BGSU portion of the work was supported by the AFOSR (FA9550-05-1-0276), the NSF (CHE-0719050), and the ACS-PRF (44138-AC3). The Ohio Laboratory for Kinetic Spectrometry is gratefully acknowledged for providing the facilities for ultrafast transient absorption measurements.

Supporting Information Available: Additional ground-state absorption spectra, excitation spectrum and emission intensity decay of **2**, along with the transient spectra of **1** obtained with the continuum generated in a CaF₂ crystal (PDF). This material is available free of charge via the Internet at <http://pubs.acs.org>.

IC800578H